JOURNAL OF SOLID STATE CHEMISTRY 110, 162–166 (1994)

Synthesis and Neutron Diffraction Study of Na_3WN_3 and Na_3MoN_3

P. E. Rauch and F. J. DiSalvo[1]

Department of Chemistry, Cornell University, Ithaca, New York 14853

and

N. E. Brese, D. E. Partin, and M. O'Keeffe

Department of Chemistry, Arizona State University, Tempe, Arizona 85287

Received May 13, 1993; in revised form August 19, 1993; accepted August 23, 1993

We have used our ambient pressure method for the synthesis of ternary alkali metal nitrides to synthesize a new class of nitrides, Na_3MN_3 (M = Mo or W). These compounds were synthesized from the metal nitride and $NaNH_2$ at 500°C under flowing ammonia at atmospheric pressure. The structures were examined using X-ray powder diffraction and neutron powder diffraction and were found to be identical with that obtained from the single crystal prepared at high pressure by Ostermann, Zachwieja, and Jacobs. © 1994 Academic Press, Inc.

INTRODUCTION

With our discovery of ambient pressure syntheses of the alkali metal tantalum nitrides and the previously unreported niobium analogs (1), we have continued our investigation to see if other alkali metal transition metal nitrides could be formed. We report here syntheses and powder diffraction studies of two alkali metal transition metal nitrides, Na_3WN_3 and Na_3MoN_3, made as polycrystalline powders at ambient pressure. We were not able to solve the structure of these two compounds until we used the recently reported single crystal structure of Na_3MoN_3, synthesized under high pressure ammonia, as a starting point for the refinements (2).

EXPERIMENTAL

All X-ray powder diffraction patterns were taken on an XDS 2000 powder diffractometer (Scintag Inc., Santa Clara, CA) using Cu$K\alpha$ radiation. Time-of-flight neutron diffraction data were collected at room temperature on the High Intensity Powder Diffractometer (HIPD) of the LANSCE facility at Los Alamos National Laboratory. Data from the $2\theta = \pm 153°$ and $\pm 90°$ detector banks were refined with the Generalized Structure Analysis System (GSAS) (3), a Rietveld profile analysis code (4). The minimum d-spacing included in the refinements was 0.66 Å unless otherwise stated. Below this point, the profiles were featureless because the reflections were broad, and more than 350 reflections contributed to each profile point.

Starting materials, WO_3 (99.99%, Atomergic, Farmingdale, NY) and MoO_3 (99.9%, Cerac, Milwaukee, WI) were used as received, without further purification. Sodium metal (99.9%, Strem, Newburyport, MA) was washed three times with hexane. All reagents and products were stored and manipulated in an argon-filled glove box, unless otherwise noted.

W_2N was synthesized by reduction of WO_3 using dry ammonia gas. In the ammonia flow, WO_3 was heated to 700°C over 6 hr and then left at 700°C for 11 hr. X-ray powder diffraction showed the product to be approximately 95% W_2N, the remainder being tungsten metal. Mo_2N was synthesized in a fashion similar to W_2N (5). X-ray powder diffraction indicated pure Mo_2N.

Na_3WN_3 was synthesized from sodium metal and W_2N in three steps. The first step formed the Na_3WN_3 and removed most of the excess $NaNH_2$ by sublimation. The second step removed the last traces of $NaNH_2$, and also caused the Na_3WN_3 to lose some of its sodium. The final step replaced the small sodium deficiency of the Na_3WN_3, through the gas phase, and therefore did not introduce any excess $NaNH_2$.

Typically, 3.84 g (0.0101 mole) of W_2N was loaded into a large alumina boat. An excess of sodium metal, with the thin oxide coat cut away, typically 3.65 g (0.159 mole), was also placed into the alumina boat. A small piece of sheet copper metal was placed completely over the boat, to prevent any devitrified pyrex or quartz from falling into the reaction mixture. This assembly was placed into a pyrex tube, and then allowed to react with dry ammonia gas, as previously described. The reaction mixture was

[1] To whom correspondence should be addressed.

0022-4596/94 $6.00
Copyright © 1994 by Academic Press, Inc.
All rights of reproduction in any form reserved.

quickly heated to 50°C, and then over 1 hr, heated to 350°C, to begin the formation of $NaNH_2$ from the sodium metal and the ammonia gas. Over the next 3 hr the sample was heated to 500°C, to complete the formation of the $NaNH_2$. Next, the sample was allowed to soak at 500°C for 8 hr to complete the formation of Na_3WN_3. Finally, the sample was allowed to cool in the furnace.

In the second step, the alumina boat, with the copper shield, was moved to a quartz tube and again allowed to react with dry ammonia gas. The sample was immediately heated to 50°C, and over the course of 2 to 3 hr heated to 600°C, then left to soak at 600°C for 8 hr, and finally cooled in the furnace.

In the final step, the alumina boat with the copper shield was moved to a pyrex tube. A small piece of oxide-free sodium metal (~0.4 g) in an alumina boat was placed upstream of the orange-yellow reaction mixture. With dry ammonia gas flowing, the sample was immediately heated to 50°C, and over the course of 1 hr heated to 350°C, and then heated to 500°C over the next 3 hr. $NaNH_2$ then sublimed over the main reaction mixture for 8 hr at 500°C. Finally, the reaction mixture was allowed to cool in the furnace.

The final product was bright yellow, and the X-ray powder diffraction pattern showed only a very small amount of WN (less than 1%) as an impurity. Neutron powder diffraction also found traces of minor phases. Elemental analysis was performed by atomic emission from an inductively coupled plasma (ICP)[2].

The Na_3MoN_3 was made in the same manner as Na_3WN_3, using Mo_2N instead of W_2N, except that before the final step, the sodium-deficient Na_3MoN_3 was ground in a mortar and pestle. The final product was maroon red, and again, the X-ray powder diffraction pattern showed only a very small amount of MoN (less than 1%) as an impurity.

RESULTS AND DISCUSSION

The syntheses of Na_3WN_3 and Na_3MoN_3 are significantly more complex than that of $NaTaN_2$ or $KTaN_2$. As previously described (1), the syntheses of $NaTaN_2$ and $KTaN_2$ consist of a single step, combining the formation of the alkali metal amide, synthesis of the product phase, and removal of any excess alkali metal amide. With Na_3WN_3 and Na_3MoN_3, the first two steps are combined, but the removal of the excess alkali metal amide is not as simple, for two reasons. First, all the excess amide cannot be removed at 600°C in a reasonable period of time, without removing the reaction mixture from the original reaction tube. The reasons for this are not completely clear, but may have to do with the inclusion of the copper shield, and the reduced temperature of amide removal, both combining to reduce the rate of amide sublimation. By removing the reaction mixture to a clean tube, any previously sublimed amide is eliminated, apparently increasing the initial sublimation rates.

The second complicating factor is that all the excess alkali metal amide cannot be sublimed out without a simultaneous loss of sodium from Na_3WN_3 and Na_3MoN_3. Hence, once all the amide is removed, the lost sodium must be replaced by a gas phase reaction. If the amide is removed at higher temperatures (700°C), then either too much sodium is lost to replace by a gas phase reaction, or the sodium loss is simply irreversible.

These compounds can also be synthesized from the corresponding transition metal and sodium amide. As in the case of $MM'N_2$ (M = Na or K, M' = Ta or Nb) (1), the newly forming compound blocks further reaction with the interior of the metal particle, preventing complete reaction without many grinding and re-reaction steps. It should be noted, however, that even with the use of the transition metal nitride, a small amount of unreacted nitride is still found. Unlike $LiMoN_2$, these phases could not be synthesized from oxide precursors, Na_2WO_4 or Na_2MoO_4, under flowing ammonia (6). Rather, these oxide precursors form oxynitrides, Na_3MO_3N (M = W or Mo) (7).

Ostermann, Zachwieja, and Jacobs recently reported the structure of Na_3MoN_3 (2) (Table 1), and this was used as a starting model in our studies. It was expected that the N positions and displacement parameters from a neutron structure determination would be more reliable. However, the low symmetry and broad peaks exhibited by this material, probably caused by small particle size, precluded a definitive structural determination.

Several refinement schemes were employed. The background was modeled using a cosine series, and the peak shapes were modeled using the Von Dreele–Jorgensen–Windsor function (8). In addition, the diffractometer zero points, lattice parameters, and absorption coefficients (9, 10) were included in the refinements. The results of several attempts are listed in Table 2.

We first tried a fixed-model refinement based on the previous structure determination (2). Only the lattice parameters, background coefficients, diffractometer zero point, and the Gaussian width of the peaks (σ_1) were refined. This refinement converged and served as a reference; that is, it measures how well the known structure of Na_3MoN_3 matches our neutron data for Na_3WN_3. The residuals $\chi^2 = 3.195$, $wR_p = 0.071$, and $R_p = 0.048$ as well as the observed and calculated histograms (see Fig. 1)

[2] The elemental analysis gave tungsten 64.5% (62.4% expected) and nitrogen 14.1% (14.3% expected). The sodium content was found to be 27.9% (23.4% expected). Because the sodium value is high, without a simultaneous reduction of the nitrogen and tungsten values, and because of the ubiquitous nature of sodium, we have discounted its anomalously high value.

TABLE 1
Atomic Positions and Neutron Scattering Lengths of Na_3MoN_3 (2)

Space group *Cc*, $Z = 8$, $a = 13.854(5)$ Å, $b = 10.889(2)$ Å, $c = 6.366(2)$ Å, $\beta = 117.23(3)°$

Position	Atom	x	y	z	b (10^{-12} cm)
4a	Mo(1)	0	0.23793(8)	0	0.66
4a	Mo(2)	0.25034(9)	0.2511(1)	0.5752(2)	0.66
4a	N(1)	0.004(1)	0.393(1)	0.906(3)	0.94
4a	N(2)	0.022(1)	0.126(2)	0.822(4)	0.94
4a	N(3)	0.242(1)	0.384(2)	0.735(3)	0.94
4a	N(4)	0.2920(9)	0.127(1)	0.781(2)	0.94
4a	N(5)	0.605(1)	0.285(1)	0.823(3)	0.94
4a	N(6)	0.356(1)	0.290(2)	0.469(4)	0.94
4a	Na(1)	0.4918(5)	0.2163(5)	0.015(1)	0.35
4a	Na(2)	0.3806(6)	0.0206(6)	0.578(1)	0.35
4a	Na(3)	0.6249(5)	0.0201(5)	0.814(1)	0.35
4a	Na(4)	0.2379(7)	0.2483(8)	0.037(2)	0.35
4a	Na(5)	0.6173(5)	0.5256(6)	0.628(1)	0.35
4a	Na(6)	0.3641(7)	0.4864(9)	0.120(2)	0.35

are generally acceptable. However, an analysis of the residuals revealed poor agreement of the observed and calculated intensities for reflections with *d*-spacings lower than 0.75 Å (a region from which much of the structural information is derived). In addition, Fourier difference peaks as high as 5% of a N atom (30% of a Na atom) were observed.

A structure refinement with isotropic displacement parameters linked together by atom type resulted in negative U_{iso} values for both Na and W atoms. A fully free refinement left three of the fourteen U_{iso} values farther than 2σ away from positive. In addition, the structural models obtained included W–N and Na–N bond lengths as short as 1.66 and 2.12 Å, respectively.

The X-ray scattering lengths of Na and N are much smaller than Mo and W. Therefore, we tried to refine several models in which the positions of the W atoms were fixed at the values for Mo determined in the X-ray diffraction experiments.

In the first refinement, we held the W positional parameters fixed, and refined an overall U_{iso} value. The U_{iso} value refined to an acceptable value of 0.0137(6); however, short Na–N distances were again obtained (minimum of 2.24 Å), although the W–N distances were more acceptable (1.70–2.05 Å).

A refinement in which the W positional and displacement parameters were fixed but all other parameters were unconstrained resulted in two negative U_{iso} values. Unacceptably short Na–N distances were also obtained (minimum of 2.06 Å).

These refinements were all unstable and required considerable damping in the beginning cycles. Convergence was achieved slowly. The diffraction profiles were rather broad. Most of the structural information was obtained from peaks in the low *d*-spacing ranges, and there was considerable overlap of reflections in these regions (up to 350 peaks contributed to a single profile point) due to the low crystallographic symmetry. This problem was exacerbated by the presence of some unidentified minor phases. Therefore, we were not able to improve upon the structural information obtained in the previous X-ray diffraction experiment.

The most notable features of the structure of Na_3WN_3 are the continuous chains of WN_4 tetrahedra (see Fig. 2). The two bridging N atoms (shared between tetrahedra) form long bonds to the W atoms, while the terminal N

TABLE 2
Refinement Schemes

Feature of refinement	Variables	R_p	wR_p	χ^2
No model refined	66	0.048	0.071	3.195
U linked by atom type	111	0.034	0.052	1.808
Fixed W positions	114	0.036	0.057	2.105
Fixed W, overall *U*	103	0.038	0.061	2.121
Completely free	122	0.033	0.052	1.775

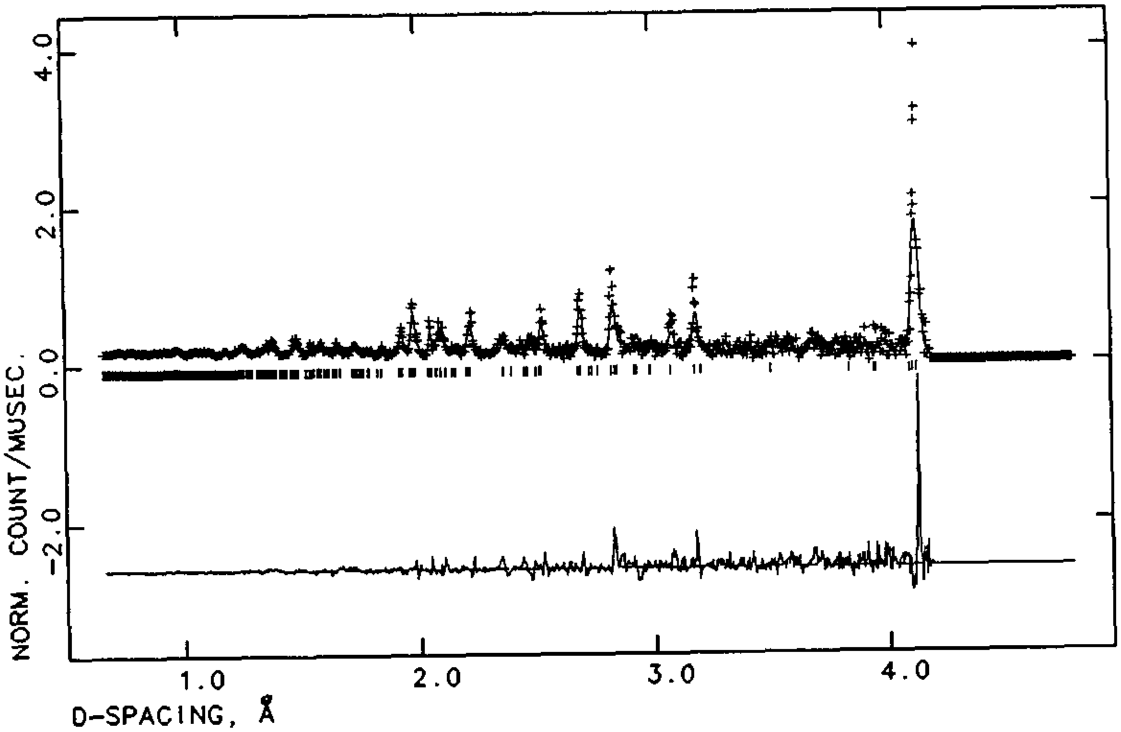

FIG. 1. Observed (+) and calculated (solid line) histograms from a fixed-model refinement based on the previous structure determination (2). The difference profile at the bottom of the figure is on the same scale.

atoms form relatively short (strong) bonds, as expected from classical ideas of crystal chemistry. Ostermann has noted that the WN_4 chains may be described with the Zintl–Klemm concept (2).

The bond-valence method has been promoted as a tool for crystal chemists (11) and has been applied to nitrides (12). The basic tenet of the method is that associated with each bond length is a unique bond valence (strength) such that the sum of all the individual bond valences is equal to the atom's total valence. This method of partitioning of an atom's bonding power into individual bonds makes use of an empirical equation to quantify bonding in crystals. Bond-valence parameters appropriate to nitrides are available (13), and we have applied them to the structure of Na_3MoN_3.

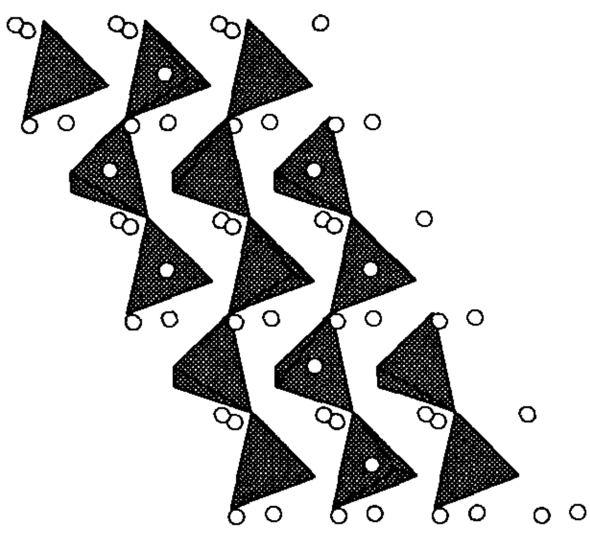

FIG. 2. View of Na_3WN_3 looking down the *b* axis. The circles represent sodium atoms. The vertices of the tungsten-centered tetrahedra represent nitrogen atoms.

At first glance, the tetrahedra in Na_3WN_3 might be expected to contain W–N bonds of 3/2 valence units (v.u.), since the sum at W would then be 6 v.u. This assignment would leave the bridging N atoms with a sum of 3 v.u. and the terminal N atoms each with a bonding of 3/2 v.u. to form Na–N bonds. However, the Na atoms use some of the bonding power of the bridging N atoms, thus weakening the W–N bonding. To maintain a total of 6 v.u. for the W atoms, the bonding to the terminal N atoms is strengthened (v(terminal) = 1.90–2.00 v.u., v(bridging) = 1.25–1.40 v.u.). A complete listing of bond valences and electrostatic energies (calculated using the method of Ewald (14)) is given in Table 3. The average deviation of the valences from their expected values is excellent.[3]

We attempted to optimize the structure of Na_3MoN_3 subject to bond valence and bond length constraints using the DVLS program (15). However, as expected from the good match of valence sums and expected valences, the

[3] $\langle |\nu - \Sigma \nu_i| / \nu \rangle = 0.08$.

TABLE 3
Bond Valences and Electrostatic Energies

Atom	$\Sigma \nu_i$	Madlung potential (V)
Na(1)	0.73	−10.98
Na(2)	1.04	−14.22
Na(3)	0.94	−13.47
Na(4)	0.79	−10.44
Na(5)	0.94	−13.41
Na(6)	0.95	−13.70
Mo(1)	6.64	−61.47
Mo(2)	6.53	−60.93
N(1)	2.90	33.60
N(2)	3.15	34.52
N(3)	2.96	33.72
N(4)	3.20	34.49
N(5)	3.14	41.64
N(6)	3.20	41.62

structural model changed insignificantly. A "better" starting model for the refinement is, therefore, not available.

The structure is somewhat surprising from the stoichiometry given that the favored coordination environment for N is an octahedron (12). The coordination numbers $^{iv}Na_3{}^{vi}W^{vi}N_3$ would offer a more symmetrical structure than the observed $^{v}Na_2{}^{iv}Na^{iv}W^{vi}N_3$, where the preceding roman numerals in superscript indicate coordination number. This observation suggests that the role of Na in the compound is not one of passive electron donor but rather one of active participant in the bonding.

In the only other tungsten (VI) and molybdenum (VI) nitrides known, Ba_3MN_4 (M = Mo or W), the transition metal is also tetrahedrally coordinated, but these tetrahedra are isolated (16). In Ca_3CrN_3 the chromium atom is only trigonally coordinated (17). Another interesting comparison is one with oxides. Many ternary oxides of molybdenum (VI) and tungsten (VI) contain the transition metal in a tetrahedral site, such as $CaMoO_4$ (sheelite structure), Li_2WO_4 (phenacite structure), and Cs_2WO_4 (β-K_2SO_4 structure) (18). On the other hand, it is interesting to note that in the more covalent binary oxides, MoO_3 and WO_3, the transition metal is octahedrally coordinated by oxygen. Perhaps if "WN_2" or "MoN_2" could be made, the transition metal might be six-fold coordinated.

It should be noted that we have not simply substituted ammonia at ambient pressure for *nitrogen* at high pressure, but rather for *ammonia* at high pressure. This shows that Na_3MoN_3 and Na_3WN_3 (like $KTaN_2$ and $NaTaN_2$ (1)) are not high pressure phases kinetically trapped at low pressure. In many cases it appears that high pressure is not necessary to prepare phases first reported using this method. High pressure, however, does seem to stabilize these phases at higher temperature, and this may be why previous preparations (2) have yielded larger crystals. The broad peaks exhibited by this material with atmospheric pressure preparation are likely caused by small crystallite size.

CONCLUSION

By extending our ambient pressure method for the synthesis of ternary alkali metal nitrides, we have synthesized Na_3WN_3 and Na_3MoN_3 from the corresponding transition metal sub-nitride and $NaNH_2$ at 500°C, under flowing ammonia. We have also confirmed the previously reported structures of these compounds using neutron diffraction. Finally, we have examined the structures of these compounds by using the bond-valence method and by comparison to other related compounds.

ACKNOWLEDGMENTS

We greatly appreciate the support of the Office of Naval Research. We also thank Mike Rudsky for assistance with the elemental analysis. The research at ASU was supported by NSF grant DMR 9120191.

REFERENCES

1. P. E. Rauch and F. J. DiSalvo, *J. Solid State Chem.* **100,** 160 (1992).
2. D. Ostermann, U. Zachwieja, and H. Jacobs, *J. Alloys Comp.* **190,** 137 (1992).
3. A. C. Larson and R. B. Von Dreele, Generalized Structure Analysis System, MS-H805, Los Alamos National Laboratory, Los Alamos, NM 87545, 1990.
4. H. M. Rietveld, *J. Appl. Crystallogr.* **2,** 65 (1969).
5. C. H. Jaggers, J. N. Michaels, and A. M. Stacy, *Chem. Mater.* **2,** 150 (1990).
6. S. H. Elder, L. H. Doerrer, F. J. DiSalvo, J. B. Parise, D. Guyomard, and J. M. Tarascon, *Chem. Mater.* **4,** 928 (1992).
7. S. H. Elder, F. J. DiSalvo, J. B. Parise, J. A. Hriljac, and J. W. Richardson, Jr., *J. Solid State Chem.*, in press.
8. R. B. Von Dreele, J. D. Jorgensen, and C. G. Windsor, *J. Appl. Crystallogr.* **15,** 581 (1982).
9. K. D. Rouse, M. J. Cooper, and A. Chakera, *Acta Crystallogr. Sect. A* **26,** 682 (1970).
10. A. W. Hewat, *Acta Crystallogr. Sect. A* **35,** 248 (1979).
11. I. D. Brown, *Acta Crystallogr. Sect. B* **48,** 553 (1992).
12. N. E. Brese and M. O'Keeffe, *Struct. Bonding Berlin* **79,** 307 (1992).
13. N. E. Brese and M. O'Keeffe, *Acta Crystallogr. Sect. B* **47,** 192 (1991).
14. P. P. Ewald, *Ann. Phys. Leipzig* **64,** 253 (1921).
15. H. Kroll, H. Maurer, D. Stöckelmann, W. Beckers, J. Fulst, R. Krüsemann, T. Stutenbäumer, and A. Zingel, *Z. Kristallogr.* **199,** 49 (1992).
16. A. Gudat, P. Höhn, R. Kniep, and A. Rabenau, *Z. Naturforsch. B* **46,** 566 (1991).
17. D. A. Vennos, M. E. Badding, and F. J. DiSalvo, *Inorg. Chem.* **29,** 4059 (1990).
18. A. F. Wells, "Structural Inorganic Chemistry." Clarendon Press, Oxford, 1984.